



Active elastic metamaterials with applications in vibration and acoustics

Simon A. Pope^{a)}

Hatim Laalej^{b)}

Department of Automatic Control and Systems Engineering, University of Sheffield, Mappin Street, Sheffield, S1 3JD, UK

Steve Daley^{c)}

Matthew Reynolds^{d)}

Institute of Sound and Vibration Research, University of Southampton, Highfield, Southampton, SO17 1BJ, UK.

Elastic metamaterials provide a new approach to solving existing problems in vibration and acoustics. They have also been associated with novel concepts such as acoustic invisibility and subwavelength imaging. To be applied to many of the proposed applications a metamaterial would need to have the desired mass density and elastic moduli over a prescribed frequency band. Importantly active metamaterials provide a degree of adaptability. This paper will focus on extending a previous theoretical concept to a more realistic experimental design. This will include a consideration of the problems which arise when the theory and simulation are developed into an experimental demonstration, including the role which the control system dynamics play in the achievable performance. The adaptability of the bandwidth in which the properties achieve their desired values will also be investigated.

^{a)} email: s.a.pope@sheffield.ac.uk

^{b)} email: h.laalej@sheffield.ac.uk

^{c)} email: S.Daley@soton.ac.uk

^{d)} email: M. Reynolds @soton.ac.uk

1 INTRODUCTION

The concept of a metamaterial was first proposed in the field of electromagnetics [1-2] and subsequently extended to the fields of acoustics and elastodynamics [3-6]. Metamaterials have a number of important properties such as a subwavelength structure and the ability to provide a material with negative values for its effective constitutive parameters, which are the mass density ρ and elastic moduli κ of the material for elastic materials. It is well known that when the mass density and elastic moduli of a material have opposite signs, the material partially blocks the propagation of any wave within the material. On the other hand, when both of these parameters have the same sign, wave motion is permitted. If both parameters are positive, the wave motion is as expected in a conventional material. However, if both parameters are negative, the refractive index $n = \pm\sqrt{\rho/\kappa}$ of the material becomes negative real. As a result, any wave moving from a material with a positive real to one with a negative real refractive index will experience negative refraction, i.e., the refracted wave will lie on the opposite side of the boundary normal to the conventional case. This is still in agreement with Snell's law.

Previous studies have designed elastic metamaterials that achieve the objective of a single negative effective parameter. For example, a negative effective mass density can be realized through an array of dipolar resonances contained within a host or attached to a transmission material. Examples include an array of lead spheres coated with a silicone rubber and embedded in an epoxy host [4], resonant masses connected through a spring element periodically along a transmission medium composed of a series of mass and spring elements [7] and mass-spring resonators periodically attached to a slender beam [5]. In these materials the result is a negative effective mass density associated with the fundamental resonant frequency of the embedded or attached elements. Alternatively, a negative effective modulus can be realized through an array of monopolar resonances. An example is a material with an array of split hollow spheres embedded within a sponge matrix [8]. This design was subsequently extended to demonstrate that a multi-band and potentially broadband response can be achieved by varying the dimensions of the split hollow spheres [9].

The majority of previous research has focused on achieving a single negative parameter, which is partly due to the difficulty in achieving simultaneously negative mass density and elastic modulus. However, several studies have proposed designs for simultaneously double negative metamaterials. An active elastic metamaterial design was proposed whereby the motion of one-dimensional array of resonant masses was controlled by a feedback control system, leading to an effective system with a frequency band in which the mass and stiffness were both negative [14]. A subsequent study proposed a passive metamaterial design with both negative effective mass density and modulus [10]. The system consisted of locally resonant translational and rotational inertia coupled by an arrangement of springs. This design enables the system to achieve a narrow frequency band over which both effective modulus and effective mass are negative. The negative modulus and effective mass are due to a monopole resonance associated with the rotational inertia and a dipolar resonance associated with the translational inertia respectively. An important extension to this study is that the initial one-dimensional concept is expanded to two-dimensions and the response demonstrated in simulation. Another study also considers a two dimensional approach in which a lumped parameter system is realized through a composite elastic structure which provides monopole, dipole and quadrupole resonances leading to

dispersive properties for the effective bulk modulus, density and shear modulus respectively [11].

Passive solid elastic metamaterial designs rely on dynamic phenomena, usually in the form of spatially periodic resonant structures to realize the negative effective parameters. As a result, a fundamental problem arises. That is, the resulting effective mass density and elastic moduli are both inherently dispersive in nature and only negative over a small frequency band. Although some studies have shown that in solid elastic materials it is possible to achieve a wide frequency band in which one of the effective parameters is negative, the simultaneously double negative frequency band, in many cases, is limited by the narrow band of the other negative effective parameter [10-11]. However in some cases, it may be possible to extend these approaches such that the double negative frequency band broadens [9], but due to the dispersive nature of the effective parameters the resulting negative effective refractive index is dispersive. This may not be a problem in applications where only a fixed narrow band response is required, as the dispersion maybe limited over this band, but it may limit the application of these designs to many of the interesting applications which have been proposed for metamaterials, such as invisibility cloaks [12] and subwavelength resolution lenses [13].

Active metamaterials can potentially overcome some of the limitations of passive designs. The previously proposed novel active elastic metamaterial (AEM) design applied non-collocated control forces to an array of single resonant units, in order to provide a system which emulates the monopole and dipole behavior required by an effective system with negative effective values for the bulk modulus and density [14]. The advantage of such an arrangement is that the control parameters can be tuned so that the double negative frequency band and transmission properties can be designed for a particular application, or potentially adapted online. They also provide a mechanism whereby designs can be realized which cannot otherwise be achieved using passive components. However, the previous work was purely theoretical and ignored important elements which need to be considered if the design is to be realized experimentally and potentially used in practical applications. These elements include the actuators needed to implement the non-collocated control forces and importantly the stability of the proposed AEM. In this paper both the stability and performance of the previously proposed AEM is analyzed in simulation when the control forces are realized by the two commonly used actuators, namely inertial and reactive actuators. This provides an important basis for the experimental demonstration of the theoretical results of the previous study

2 COMPARATIVE DESIGNS FOR AN AEM WITH INERTIAL AND REACTIVE ACTUATORS

The theoretical design for an AEM proposed in a previous study assumed that an inertial force could be applied directly to the resonant masses as described in figure 1. However, realizing the inertial force in figure 1 is not straightforward and requires the use of a particular type of actuator. The inertial actuator generates a control force f_c by reacting its inertial system comprising of mass m_a , stiffness c_a and damping k_a against a controlled structure m_b as shown in figure 2 (a). As such the control force, which can be described by equation (1) where s is the Laplace operator, is a function of the mechanical dynamics of the actuator. In addition the actuator force f_a is also a function of the electrical characteristics of the force generation mechanism. It is well reported in active control literature that the inclusion of these dynamics

into active vibration system can often results in an unstable system [15-17]. The inclusion of these inertial actuator dynamics into the previously proposed theoretical AEM has been investigated and shown that the control system employed, has to be extended from its original structure to compensate for the actuator dynamics to ensure both a simultaneously double negative region in the frequency response and a stable system [18].

$$f_c = -\frac{m_a s^2 (c_a s + k_a)}{m_a s^2 + c_a s + k_a} x_b - \frac{m_a s^2}{m_a s^2 + c_a s + k_a} f_a \quad (1)$$

In active vibration control, there are two widely used actuators namely reactive and inertial actuators. In contrast to the inertia actuator which is normally placed on top of the structure that needs to be controlled and has no other connections, the reactive actuator is normally placed between the structure to be controlled and a base structure. The basic operation of the reactive actuator is to generate a control force f_a that reacts against a controlled structure m_b as shown in figure 2 (b). As such the control force generated by a reactive actuator, which can be described by equation (2), doesn't include any mechanical actuator dynamics. Although active vibration systems with reactive actuators are well known to be unconditionally stable for collocated control forces, active systems can become unstable under non-collocated control forces [15].

$$f_c = -f_a \quad (2)$$

Figure 3 shows an alternative design to that previously investigated, whereby the inertial control force of Figure 1 has been replaced by a control force generated by a reactive actuator which is attached to a fixed foundation. Otherwise the structure of the AEM is identical to that in Figure 1. The potential advantage of the arrangement in Figure 3 is that the control force doesn't suffer from significant mechanical dynamics inherent in the actuators design. The disadvantage is that it requires each of the reactive actuators to be attached to fixed points, thereby reducing the flexibility in the physical design of the system.

The equation of motion of the AEM with reactive actuators can readily be described by equation (3).

$$M\ddot{X} + C\dot{X} + KX = F \quad (3)$$

where

$$M = \begin{pmatrix} m & 0 & \cdots & 0 \\ 0 & m_r & 0 & \\ \vdots & 0 & \ddots & 0 \\ & & & 0 & m & 0 \\ 0 & \cdots & 0 & m_r \end{pmatrix} \quad C = \begin{pmatrix} c+c_r & -c_r & -c & \cdots & 0 \\ -c_r & 2c_r & 0 & \cdots & 0 \\ 0 & \ddots & \ddots & \ddots & \vdots \\ \vdots & -c & 0 & c+c_r & -c_r \\ 0 & \cdots & 0 & -c_r & 2c_r \end{pmatrix}$$

$$K = \begin{pmatrix} k+k_r & -k_r & -k & \cdots & 0 \\ -k_r & 2k_r & 0 & \cdots & 0 \\ 0 & \ddots & \ddots & \ddots & \vdots \\ \vdots & -k & 0 & k+k_r & -k_r \\ 0 & \cdots & 0 & -k_r & 2k_r \end{pmatrix}$$

are the mass, damping and stiffness matrices respectively and

$$X = \begin{pmatrix} x_1 \\ x_{r_1} \\ \vdots \\ x_n \\ x_{r_n} \end{pmatrix} \quad F = \begin{pmatrix} f_1 \\ f_{a_1} \\ \vdots \\ f_n \\ f_{a_n} \end{pmatrix}$$

3. STABILITY AND PERFORMANCE ANALYSES OF THE AEM WITH REACTIVE ACTUATORS

In the previous study it was demonstrated theoretically that the AEM in figure 1 under the non-collocated control scheme of equation (4) can achieve the simultaneously double negative parameters required for negative refraction in a prescribed frequency band. This assumed perfect control, i.e. the control system dynamics could be ignored.

$$f_{c_i} = (c_c s + k_c)(x_{i-1} + x_{i+1} - 2x_{r_i}) \quad \text{for } i = 1, \dots, n \quad (4)$$

The simplest control scheme which provides the system in figure 1 with the double negative parameters is one which is based on a pure displacement feedback, i.e. $c_c = 0$ in equation (4). For simplification of the analysis, this simplest control scheme will be adopted in the present study. In this case, the force generated by the reactive actuator in equation (2) can be rewritten as:

$$f_c = -f_a = k_c(x_{i-1} + x_{i+1} - 2x_{r_i}) \quad \text{for } i = 1, \dots, n \quad (5)$$

3.1 Stability analysis of the AEM with reactive actuators

The AEM described by equation (3) is essentially a multivariable system. It has $2n$ inputs (n control actuator inputs and n transmission inputs) and $2n$ outputs (the displacements of the transmission and resonant masses). If the system is assumed to be closed, i.e. bounded at either end by a ‘‘disturbing medium’’ this reduces to $n+2$ inputs (n control actuator inputs and 2 disturbance inputs). Re-arranging the equations of motion in equation (3) so that the system can be expressed as a state space model with inputs $\vec{u} = [\vec{f}, \vec{f}_d]^T$ where \vec{f} and \vec{f}_c are the vectors of

control forces applied to the transmission and resonant masses respectively and outputs $\bar{y} = [\bar{x}, \bar{x}_r]^T$ where \bar{x} and \bar{x}_r are vectors of displacements of the transmission and resonant masses respectively, the feedback control inputs can be expressed in matrix form as in equation (6).

$$G_c = -k_c K_c = -k_c \begin{bmatrix} K_{c_{1,1}} & K_{c_{1,2}} \\ K_{c_{2,1}} & K_{c_{2,2}} \end{bmatrix} \quad \text{such that} \quad [0, \bar{f}_c]^T = G_c \bar{y} \quad (6)$$

The four sub matrices of K_c are all $n \times n$ matrices with $K_{c_{1,1}}$ and $K_{c_{1,2}}$ both zero matrices, $K_{c_{2,1}}$ a zero matrix except for 1's on the two diagonals either side of the leading diagonal and the two end elements of the leading diagonal and $K_{c_{2,2}}$ is the zero matrix with -2 of the leading diagonal except for -1 on the elements at both ends of the diagonal. The closed loop response of the AEM with reactive actuators can then be determined from $\bar{y} = (I - GG_c)^{-1} G \bar{f}$, where G is the open loop response obtained from the state space form of equation (3). Analyzing the stability of the AEM with reactive actuators is not trivial due to its multivariable nature. However, it is well known that internal stability of a multivariable system is guaranteed if $(I - GG_c)^{-1}$ is stable and there are no right half plane pole-zero cancellations between G and G_c . As G is stable due to its passive construction, the requirement is whether there are any right half plane zeros in G which cancel with right half plane poles in G_c . The non-collocated controller in equations (6) has no poles and therefore it cannot cancel any right half zeros present in the plant G . As a result, the stability of the system can be inferred directly from the analysis of the roots of $(I - GG_c)^{-1}$ using well known stability analysis tools. Figure 4 shows the movement of the closed loop poles of a fourth order system $n = 4$ (i.e. four transmission masses) with the parameters $m = 5Kg$, $k = 5 \times 10^4 N/m$, $c = 0.1Ns/m$, $m_r = 2Kg$, $k_r = 8 \times 10^3 N/m$ and $c_r = 2 \times 10^{-3} Ns/m$ when the controller gain k_c is varied from zero to an upper cut-off. These system parameters are chosen from a proof of concept perspective and are not necessarily indicative of any particular application. The trajectory of the closed loop poles in figure 4 indicates that the AEM with reactive actuators is stable over the range of feedback gain $k_c \in [0, 16000]$. for the given system.

3.2 Performance analysis of the AEM with reactive actuators

The requirement for a negative refractive index in an AEM is that both the effective mass and stiffness are simultaneously negative over a frequency range of interest, whilst ensuring that the system is also stable. The objective of this section is therefore to investigate the performance of the AEM with reactive actuators shown in figure 3 using a stable feedback gain. The effective equation of motion for mass i can be written as equation (7), where the effective mass and stiffness are given by equations (8) and (9) respectively.

$$m_e x_i s^2 = (c_e s + k_e)(x_{i-1} + x_{i+1} - 2x_{r_i}) \quad (7)$$

$$m_e = m + \frac{(c_r s + k_r)(s^2 m_r + (c_r s + k_r))}{s^2 (m_r s^2 + 2c_r s + 2(k_r + k_c))} \quad (8)$$

$$c_e s + k_e = cs + k + \frac{(c_r s + k_r)(c_s s + k_s)}{m_r s^2 + 2c_r s + 2(k_r + k_c)} \quad (9)$$

The desired terms required for analysis of the effective parameters are the real parts of equations (8) and (9) which can readily be obtained as equations (10) and (11). The imaginary parts of equations (8) and (9) constitute the loss terms for the effective system.

$$\text{Re}(m_e) = m + \frac{m_r \omega^4 (-m_r k_r + 2k_c c_r + c_r^2) + \omega^2 (-2k_c (c_r^2 + k_r m_r) + k_r (2c_r^2 - 3k_r m_r)) - 2k_r^2 (k_c + k_r)}{\omega^2 (m_r^2 \omega^4 + 4\omega^2 (-m_r (k_c + k_r) + c_r^2) + (2k_c + 2k_r)^2)} \quad (10)$$

$$k_e = k + \frac{\omega^2 (-m_r k_c k_r + 2k_c c_r^2) + 2k_c k_r (k_c + k_r)}{m_r^2 \omega^4 + 4\omega^2 (-m_r (k_c + k_r) + c_r^2) + (2k_c + 2k_r)^2} \quad (11)$$

Because the denominators on the right hand side in equations (10) and (11) are the results of the multiplications of the original denominators in equations (8) and (9) by their complex conjugates, they are therefore guaranteed to be positive semi-definite. Consequently, the objective of providing negative effective mass and stiffness of the system requires the numerators of the terms in equations (10) and (11) to be negative over a specified frequency bandwidth. This leads to the two inequalities given in equations (12) and (13) to provide negative effective parameters.

$$m_r \omega^4 (-m_r k_r + 2k_c c_r + c_r^2) + \omega^2 (-2k_c (c_r^2 + k_r m_r) + k_r (2c_r^2 - 3k_r m_r)) - 2k_r^2 (k_c + k_r) < 0 \quad (12)$$

$$\omega^2 (-m_r k_c k_r + 2k_c c_r^2) + 2k_c k_r (k_c + k_r) < 0 \quad (13)$$

These two inequalities are necessary but not sufficient to ensure the effective parameters are negative. Sufficiency is achieved by also ensuring that the magnitudes of the right-hand terms in equations (12) and (13) are also greater than their respective passive transmission parameters: mass m and stiffness k , in addition to being negative. This further complicates the analysis of the effective parameters. Following the previous theoretical work, considerable insight can be found by analyzing equations (10) and (11) [14]. The denominators of these two equations have the same resonant frequency $\sqrt{(2k_c + 2k_r)/m_r}$. It is at this frequency that the magnitudes of these components will be large. Thus if the resonance is sufficiently large, negative effective parameters are guaranteed if the frequency range in which the inequalities of equations (10) and (11) overlap with the resonance frequency. They do not necessarily need to overlap with the centre point of the resonant frequency as long as the magnitudes are sufficiently larger than the passive components of the AEM.

Figure 5 shows the displacement transmission across four masses for the same system as used in Section 3.1. The feedback gain was selected as $k_c = 10000$ which falls within the previously determined stability range $[0, 16000]$. As expected from the theoretical design [14], the double negative band marked by the dotted green lines in figure 5 is located near the resonant frequency of the effective parameters which is 112 rad/s.

To clearly demonstrate this double negative band and its tunability, the real values of the effective mass and stiffness of the AEM with reactive actuator under the non-located control gain $k_c=10000$ and over the frequency range [10rad/sec, 1000rad/sec] is plotted in figure 6 (b). In addition, figure 6 (a) takes a frequency (90rad/sec) in which the parameters are simultaneously negative and plots the change in these variable against a changing control gain k_c .

It can be seen clearly from figure 6 (b) that the effective mass and stiffness of the system become simultaneously negative when the plot is in the lower left quadrant with this stable gain for a range of frequencies. On the other hand, figure 6 (a) indicates that there is also a range in the feedback gain k_c for a given frequency, in which both the parameters are simultaneously negative and can be tuned to a limited range of values

These results suggest that that the proposed AEM implemented using reactive actuators under non-located control scheme meets the stability requirement and at the same time provides a double negative region for the effective parameters and this region is tunable to some extent. This result provides an important basis for the practical application of the theoretical results reached in the previous studies. The advantage of this design over that previously investigated for a system implemented using inertial actuators [18] is that stability and simultaneously double negative properties can be achieved using a simple non-located displacement feedback controller, whereas with the inertial actuator the control system needs to be extended to a more complex form to compensate for the significant actuator dynamics. The disadvantage of the design implemented using reactive actuators is that its physical construction allows less flexibility in design as it requires fixed terminations for the array of reactive actuators.

4. CONCLUSIONS

In a previous study a novel simultaneously double negative active elastic metamaterial design (AEM) using a non-located control scheme was proposed. However, the previous study ignored important elements which need to be considered if the design is to be verified experimentally. This includes the actuators which are needed to implement the non-located control forces and the stability of the proposed AEM. In the present study, the performance and stability of the previously proposed AEM was investigated for the case when the non-located control forces are applied via reactive actuators. The results of this study show that the proposed AEM with reactive actuators meets the stability requirement and at the same time provides a simultaneously double negative region for the effective parameters which is tunable to some extent. The design potentially provides better performance and stability using a simpler control system than that implemented using inertial actuators [18], but at the expense of a less flexible physical design. Future work will aim to verify experimentally the proposed designs for AEM.

5. ACKNOWLEDGEMENTS

The authors gratefully acknowledge the support of the Engineering and Physical Science Research Council, UK through grant (EP/J003816/1).

6. REFERENCES

1. J.B. Pendry, A.J. Holden, W.J. Stewart, I. Youngs, "Extremely low frequency plasmons in metallic mesostructures", *Phys. Rev. Lett.*, 76, 4773-4776 (1996).
2. D.R. Smith, W.J. Padilla, D.C. Vier, S.C. Nemat-Nasser, S. Schultz, "Composite medium with simultaneously negative permeability and permittivity", *Phys. Rev. Lett.*, 84, 4184-4187 (2000)
3. Z.Y. Liu, C.T. Chan, P. Sheng, "Analytic model of phononic crystals with local resonances", *Phys. Rev. B*, 014103 (2005)
4. J. Li, C.T. Chan, "Double-negative acoustic metamaterial", *Phys. Rev. E*, 70, 055602 (2004)
5. G. Wang, X.S. Wen, J.H. Wen, Y.Z. Liu, "Quasi-one-dimensional periodic structure with locally resonant band gap", *J. Appl. Mech.-T. ASME*, 73, 167-170(2006).
6. N. Fang, D. Xi, J. Xu, M. Ambati, W. Srituravanich, C. Sun, X. Zhang, "Ultrasonic metamaterials with negative modulus", *Nat. Mater.*, 5, 452-456 (2006)
7. S. Yao, X. Zhou, G. Hu, "Experimental study on negative effective mass in a 1D mass-spring system", *New J. Phys.*, 10, 043020 (2008)
8. C. Ding, L. Hao, X. Zhao, "Two-dimensional acoustic metamaterial with negative modulus", *J. Appl. Phys.*, 108, 074911 (2010)
9. C. Ding, X. Zhao, "Multi-band and broadband acoustic metamaterial with resonant structures", *J. Phys. D: Appl. Phys.*, 44, 215402 (2011)
10. X.N. Liu, G.K. Hu, G.L. Huang, C.T. Sun, "An elastic metamaterial with simultaneously negative mass density and bulk modulus", *Appl. Phys. Lett.*, 98, 251907 (2011).
11. Y. Lai, Y. Wu, P. Sheng, Z.-Q. Zhang, "Hybrid elastic solids", *Nat. Mater.*, 10, 620-624 (2011).
12. G.W. Milton, M. Briane, J.R. Willis, "On cloaking for elasticity and physical equations with a transformation invariant form", *New J. Phys.*, 8, 248 (2006)
13. S. Guenneau, A. Movchan, G. Petursson, S. Ramakrishna, "Acoustic metamaterials for sound focusing and confinement", *New J. Phys.*, 7, 399 (2007)
14. S.A. Pope, S. Daley, "Viscoelastic locally resonant double negative metamaterials with controllable effective density and elasticity", *Phys. Lett. A*, 374, 4250-4255 (2010)
15. S.J. Elliott, M. Serrand, P. Gardonio, "Feedback stability limits for active isolation systems with reactive and inertial actuators", *American Society of Mechanical Engineers, Journal of Vibration and Acoustics*, 123, 250-261, (2001).

16 L. Benassi, S.J. Elliott, P. Gardonio, Active vibration isolation using an inertial actuator with local force Feedback control, *Journal of Sound and Vibration*, 276, 157–179, (2004).

17 L. Benassi, S.J. Elliott, P. Gardonio, Equipment isolation of a SDOF system with an inertial actuator using feedback control strategies, *Proceedings of the ACTIVE2002 Conference*, Southampton, UK, 15–17, July (2002).

18 S.A.Pope, H. Laalej, S. Daley, Active elastic metamaterials with applications in vibration and acoustics, *Proceedings of the Acoustics2012 Conference*, Nantes, France, 23–27 April (2012).

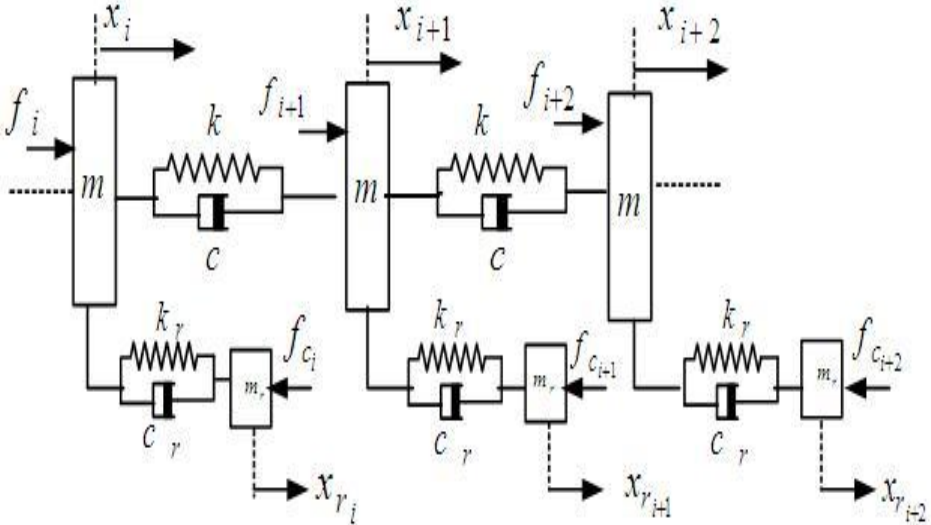


Fig. 1 – The previously proposed AEM design.

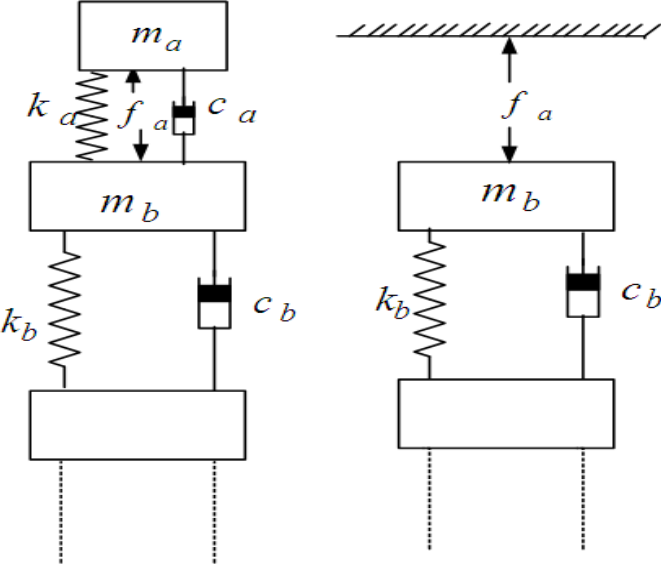


Fig. 2 – Active and reactive actuators controlling a structure with mass m_b , stiffness k_b and damping c_b : (a) Inertial actuator implementation; (b) reactive actuator implementation.

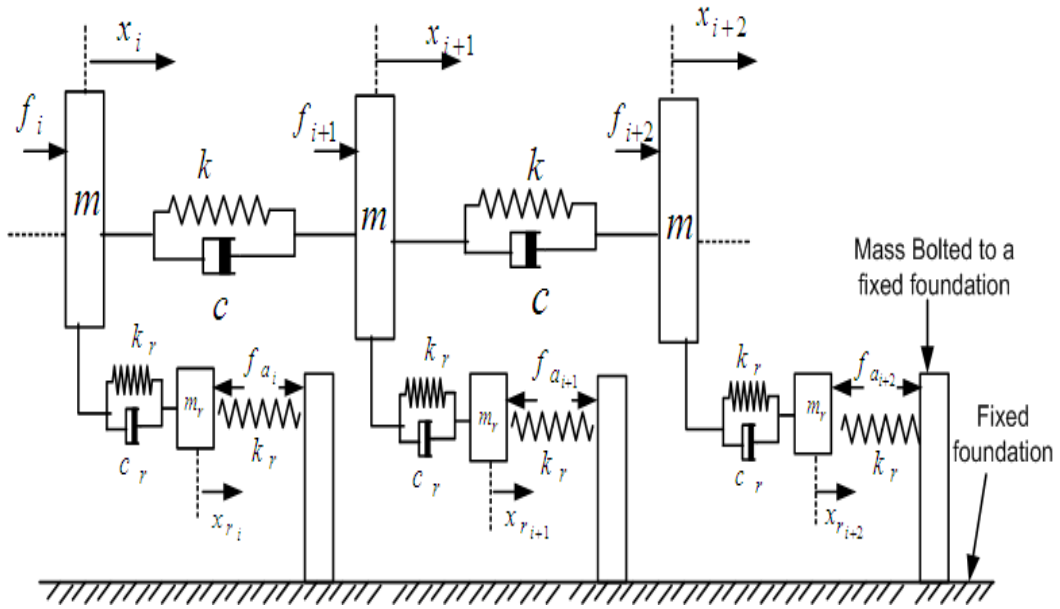


Fig. 3 – An AEM with reactive actuators.

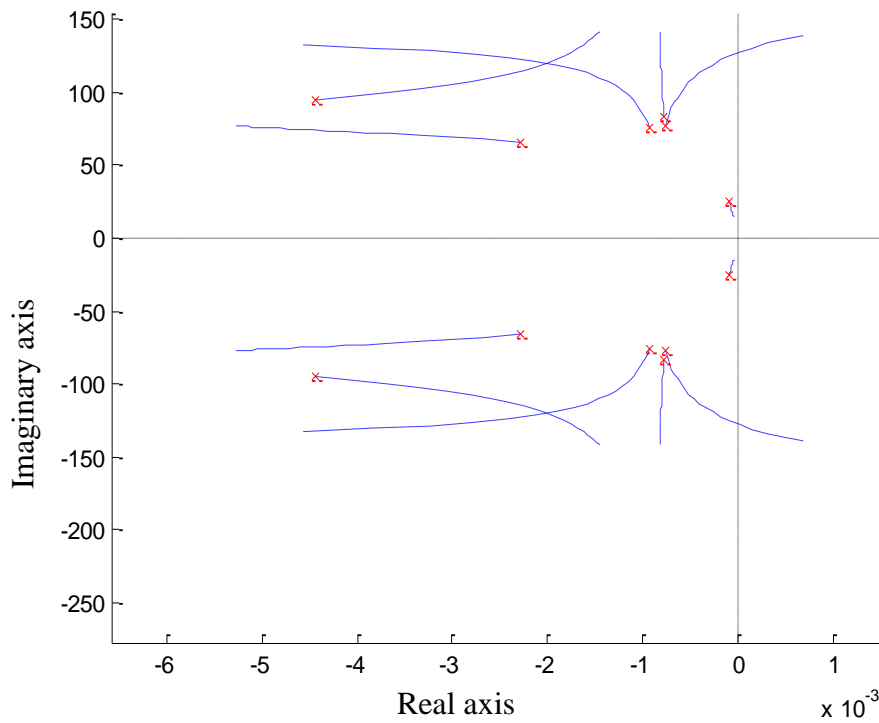


Fig. 4 – Plot of the closed loop poles with increasing feedback gain k_c of AEM with reactive actuators. The red crosses mark the poles of the open loop system, i.e. $k_c=0$.

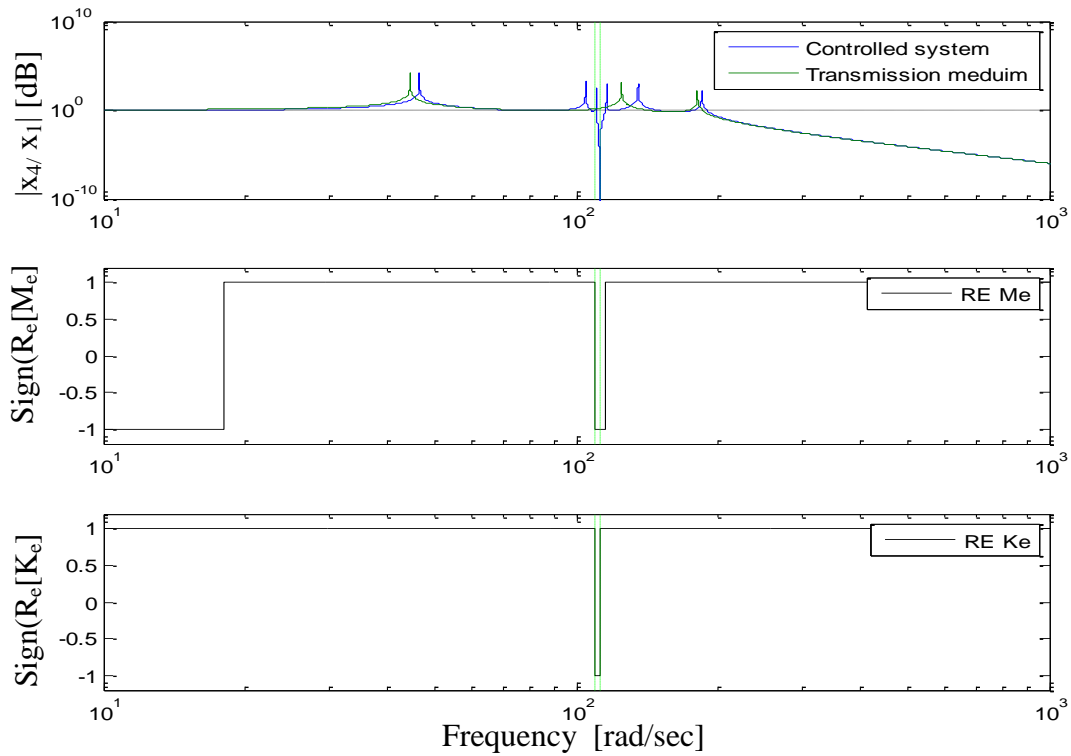


Fig. 5 – The displacement transmission across four units for the AEM with reactive actuators with $k_c=10000$.

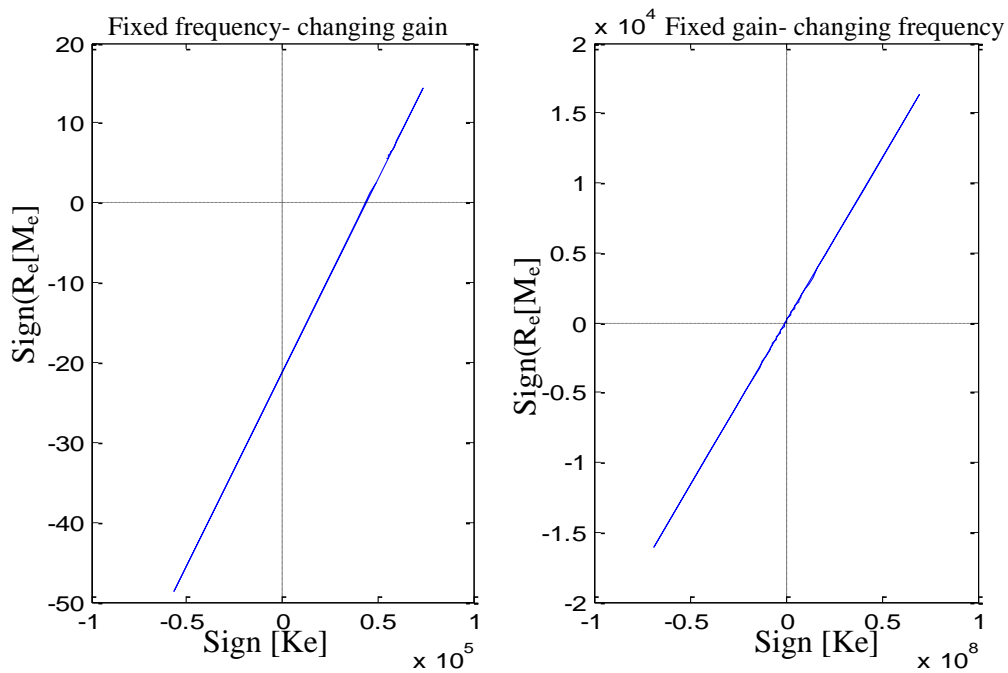


Fig.6 – Real parts of the effective mass against stiffness: (a) A fixed frequency (90rad/sec) and changing control parameters k_c ; (b) A changing frequency [10rad/sec, 1000rad/sec] and fixed control parameter k_c .